Dynamic and specific interaction between synaptic NR2-NMDA receptor and PDZ proteins

Lucie Bard[a,b], Matthieu Sainlos[a,c], Delphine Bouchet[a,b], Sarah Cousins[d], Lenka Mikasova[a,b], Christelle Breillat[a,b], F. Anne Stephenson[d], Barbara Imperiali[c], Daniel Choquet[a,b], and Laurent Groc[a,b,1]

[a]Laboratory for Cellular Physiology of the Synapse, Centre National de la Recherche Scientifique, Unité Mixte de Recherche 5091, 33077 Bordeaux, France; [b]Université de Bordeaux, 33077 Bordeaux, France; [c]Departments of Chemistry and Biology, Massachusetts Institute of Technology, Cambridge, MA 02139; and [d]School of Pharmacy, University of London, London WC1N 1AX, United Kingdom

Edited by Richard L. Huganir, The Johns Hopkins University School of Medicine, Baltimore, MD, and approved October 4, 2010 (received for review March 3, 2010)

The relative content of NR2 subunits in the NMDA receptor confers specific signaling properties and plasticity to synapses. However, the mechanisms that dynamically govern the retention of synaptic NMDARs, in particular 2A-NMDARs, remain poorly understood. Here, we investigate the dynamic interaction between NR2 C termini and proteins containing PSD-95/Discs-large/ZO-1 homology (PDZ) scaffold proteins at the single molecule level by using high-resolution imaging. We report that a biomimetic divalent competing ligand, mimicking the last 15 amino acids of NR2A C terminus, specifically and efficiently disrupts the interaction between 2A-NMDARs, but not 2B-NMDARs, and PDZ proteins on the time scale of minutes. Furthermore, displacing 2A-NMDARs out of synapses lead to a compensatory increase in synaptic NR2B-NMDARs, providing functional evidence that the anchoring mechanism of 2A- or 2B-NMDARs is different. These data reveal an unexpected role of the NR2 subunit divalent arrangement in providing specific anchoring within synapses, highlighting the need to study such dynamic interactions in native conditions.

lateral diffusion | glutamate receptor | trafficking | biomimetic multivalent ligand | development

The identification of the cellular mechanisms involved in the regulation of glutamate receptor trafficking is crucial to our understanding of synaptic maturation and plasticity. One common paradigm of these processes is the activation of the calcium-permeable postsynaptic NMDA receptors (NMDARs). In the neocortex, the most abundant types of NMDARs are composed of NR1 subunits associated with NR2A (enriched in synapses) and/or NR2B subunits (1). Rapid changes in the synaptic 2A/2B NMDAR ratio have been reported during connection refinements and synaptic plasticity (2), and several key molecular interactions have been shown to control the trafficking of intracellular and membrane NMDARs (3–6).

The intracellular proteins that interact with the C terminus of the subunits, through direct binding or modification of the phosphorylation state, are likely candidates for regulating the synaptic retention of NMDARs. Indeed, intracellular domains of NR2 subunits provide a binding motif for proteins of the postsynaptic density such as PSD-95 and SAP102 (7–10). The binding of the NR2B subunit C terminus to PDZ domain-containing scaffold proteins regulates, in part, the synaptic retention of this receptor (8, 9, 11–14). For the 2A-NMDARs, which make up the majority of synaptic NMDARs, the role of such interactions in synaptic retention remains controversial. Indeed, long-term expression of NR2A subunits with a truncated or mutated C terminus does not affect synaptic NMDAR currents in cerebellar or hippocampal neurons (9, 15), whereas deletion of the NR2A subunit C terminus sequence significantly reduces NMDAR synaptic signaling (11, 14, 16, 17). Currently, there is no simple explanation for this discrepancy, and the use of long-term expression of exogenous NR subunits and lack of good pharmacological tools to discriminate between 2A- or 2B-NMDAR signaling (18) render interpretation more difficult. Here, we apply biomimetic divalent peptide-based competing ligands to acutely interfere with the PDZ domain-containing scaffold proteins-2A-NMDAR interaction and use single quantum dot (QD) tracking to image, with subwavelength precision, the dynamics of surface synaptic NMDARs.

Results

Design of a Biomimetic Multivalent Ligand to Disrupt the Interaction Between NR2A Subunit and PDZ Domain-Containing Scaffold Proteins (PDZ Proteins). The molecular mechanisms involved in the dynamic retention of 2A-NMDARs within postsynaptic membranes are not defined. To investigate these mechanisms, we developed a peptide-based ligand that strongly and acutely perturbs the interaction between NR2A subunit and PDZ proteins (Fig. 1*A*). Similar strategies have previously been used to dissociate the PDZ scaffold–NMDAR interaction (19–21). In these studies, disruption of the PDZ protein–NMDAR interaction was achieved by using monovalent peptide sequences that corresponded to the last nine to 10 residues of a single subunit (NR2A or NR2B). We reasoned that the efficiency of such an approach could be improved by using synthetic ligands that would better mimic the native interactions. Indeed, because (*i*) NMDARs are heterodimeric complexes composed of NR2 subunit dimers and (*ii*) the scaffold proteins (e.g., PSD-95, PSD-93 and SAP-102), which interact with NMDARs, each contain clusters of PDZ domains that recognize similar targets (22), we hypothesized that a ligand composed of two NR2 C-terminal binding motifs would more efficiently dissociate the native scaffold PDZ domain–NMDAR interactions. In the current design, we conjugated two of the 15 residue C-terminal sequences of the PSD-95 NR2A binding motifs via their N-termini (Fig. S1 *A* and *B*). Homologous monovalent sequences and a previously described nonsense sequence were used as controls (Fig. S1 *A–D*) (23). A series of ligands incorporating a solvatochromic fluorophore was first used to evaluate the binding constants with recombinant PSD-95 PDZ domains 1 and 2 (23). The divalent ligand displayed a sevenfold increase of affinity for the tandem domain in comparison with the monovalent homolog (Fig. S1*C*), confirming the advantage of divalency. The ligands were then appropriately modified for specific experiments, e.g., for cell studies, by addition of a TAT cell-transduction sequence to generate TAT-$NR2A_{15}$ or TAT-$[NR2A_{15}]_2$ and/or a labeling dye (BODIPY-fluorescein).

Author contributions: F.A.S., B.I., D.C., and L.G. designed research; L.B., M.S., D.B., S.C., and L.M. performed research; M.S., C.B., and B.I. contributed new reagents/analytic tools; L.B. analyzed data; and L.G. wrote the paper.

The authors declare no conflict of interest.

This article is a PNAS Direct Submission.

[1]To whom correspondence should be addressed. E-mail: laurent.groc@u-bordeaux2.fr.

This article contains supporting information online at www.pnas.org/lookup/suppl/doi:10.1073/pnas.1002690107/-/DCSupplemental.

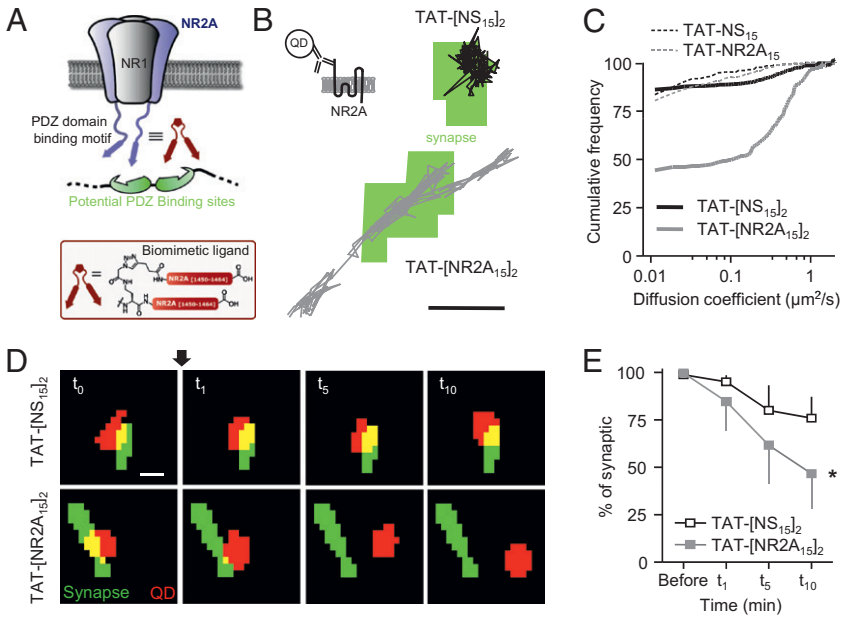

Fig. 1. Acute disruption of the interaction between 2A-NMDARs and PDZ proteins using a NR2A-derived multivalent ligand. (*A*) Schematic representation of a membrane NMDAR, a scaffold MAGUK protein, and the newly developed divalent ligand mimicking the C terminus (15 last amino acids) of two NR2A subunit subunits (TAT-$[NR2A_{15}]_2$). (*B*) Representative trajectories of surface 2A-NMDARs, based on QD-coupled antibodies against an extracellular epitope of the NR2A (*Upper Left*), after 10 to 20 min of incubation with TAT-$[NS_{15}]_2$ (*Upper*) or TAT-$[NR2A_{15}]_2$ (*Lower*). The green areas correspond to synaptic sites labeled with Mitotracker. (Scale bar: 1 μm.) (*C*) Cumulative distribution of the instantaneous diffusion coefficient of 2A-NMDARs. The first point corresponds to the percentage of immobile receptors (bin size, 0.0075 $\mu m^2/s$). Note the higher increase in the mobility of 2A-NMDARs induced by the divalent TAT-$[NR2A_{15}]_2$ ($n = 303$ trajectories; solid gray line) compared with monovalent TAT-$NR2A_{15}$ ($n = 170$; dashed gray line) or TAT-NS_{15} (dashed and solid black lines; TAT-$[NS_{15}]_2$, $n = 530$ trajectories; TAT-NS_{15}, $n = 153$ trajectories). (*D*) Displacement of individual NR2A-coupled QDs after incubation with TAT-$[NR2A_{15}]_2$. The neurons were incubated with Mitotracker (green) and NR2A-coupled QDs (red spots). The localization of NR2A-coupled QDs was followed for 10 min after acute addition (arrow) of 5 μM TAT-$[NS_{15}]_2$ (*Upper*) or 5 μM TAT-$[NR2A_{15}]_2$ (*Lower*). (Scale bar: 1 μm.) (*E*) The synaptic localization of NR2A-coupled QDs decreased over the 10 min recording after incubation with both TAT-$[NS_{15}]_2$ ($n = 11$) and TAT-$[NR2A_{15}]_2$ ($n = 6$). The reduction was significantly higher for TAT-$[NR2A_{15}]_2$ (*$P < 0.05$).

Interaction Between 2A-NMDARs and PDZ Proteins Regulates NMDAR Synaptic Retention. To investigate the ligand efficacy in neuronal preparations, hippocampal cultured neurons were incubated with a saturating (5–10 μM) nontoxic (i.e., no neuronal damage observed) concentration of TAT-$[NS_{15}]_2$ or TAT-$[NR2A_{15}]_2$. After a 10-min incubation period, neurons were efficiently labeled by the different BODIPY-containing ligands (*SI Materials and Methods*). To investigate the specific impact of the ligands on the surface 2A-NMDAR anchoring, we used single QD tracking as a high-resolution approach to estimate 2A-NMDAR surface diffusion in live neurons (24). Native 2A-NMDARs were detected by using a QD-antibody complex directed against the extracellular N terminus of the NR2A subunit (Fig. 1*B* and *SI Materials and Methods*) and their surface localization, i.e., onto a postsynaptic marker or outside synapse, determined during the recording session. The overall surface diffusion of 2A-NMDARs was increased after monovalent TAT-$NR2A_{15}$ and divalent TAT-$[NR2A_{15}]_2$ ligand incubation, although to very different extents: (*i*) the cumulative distribution of coefficient diffusion was highly shifted by TAT-$[NR2A_{15}]_2$ incubation; (*ii*) the diffusion coefficient medians were threefold and 27-fold increased by TAT-$NR2A_{15}$ and TAT-$[NR2A_{15}]_2$, respectively [i.e., TAT-$[NS_{15}]_2$ median of 4.10^{-3} $\mu m^2/s$, interquartile range (IQR) of 0–2.10^{-2} $\mu m^2/s$, $n = 530$ trajectories; TAT-$[NR2A_{15}]_2$ median of 11.10^{-2} $\mu m^2/s$, IQR of 6.10^{-4}-5.10^{-1} $\mu m^2/s$, $n = 303$ trajectories; $P > 0.05$]; and (*iii*) the fraction of mobile 2A-NMDARs (membrane diffusion >0.0075 $\mu m^2/s$) increased by 2% and 42% after TAT-$NR2A_{15}$ and TAT-$[NR2A_{15}]_2$, respectively (Fig. 1*C*). Similar results were obtained when examining solely synaptic 2A-NMDARs (Fig. S2), indicating that disruption of the 2A-NMDAR anchoring increases the fraction of mobile receptors.

To investigate the impact of TAT-$[NR2A_{15}]_2$ on identified single synaptic 2A-NMDARs, QD-2A-NMDAR complexes were tracked within synapse before and in the presence of TAT-$[NR2A_{15}]_2$ or TAT-$[NS_{15}]_2$ (Fig. 1*D*). After TAT-$[NS_{15}]_2$ incubation (10 min) the fraction of 2A-NMDARs that remained within synapses was unchanged, although a slight but not significant ($P > 0.05$) decrease is noted, consistent with the basal exchange rate of surface NMDARs between synaptic and extrasynaptic membranes (25–27). However, within the same time frame in the presence of TAT-$[NR2A_{15}]_2$, approximately half of the synaptic 2A-NMDARs escaped the synaptic area (Fig. 1 *D* and *E*), indicating that anchoring of synaptic 2A-NMDARs by PDZ scaffolds is a dynamic process. To further confirm the impact of the ligand on the surface NMDAR synaptic population, and not only single receptor, we expressed the NR1 subunit (obligatory subunit of surface NMDARs) fused to Super Ecliptic pHluorin at its extracellular N terminus (SEP-NR1) to isolate the surface fraction and quantify the average surface diffusion of SEP-NR1-containing NMDARs using fluorescence recovery after photobleaching (FRAP; Fig. S3 *A–C*). The recovery of SEP-NR1 fluorescence in dendrites was approximately 50%, whereas it was only 20% in synapses (25). Consistently, a decrease of the percentage of immobile synaptic receptors was observed, i.e., from 85% before incubation with TAT-$[NR2A_{15}]_2$ to 65% following 20 min incubation (Fig. 1*E*). The proportion of immobile receptors outside synapses was not affected, suggesting that TAT-$[NR2A_{15}]_2$ acts on synaptically enriched 2A-NMDARs (11, 28). Finally, these results were further confirmed with immunocytochemical staining of synaptic NR2A subunits (colabeled with PSD-95), as, over a large fraction of synapses (TAT-$[NR2A_{15}]_2$, $n = 1{,}684$ synapses; TAT-$[NS_{15}]_2$, $n = 1{,}981$), TAT-$[NR2A_{15}]_2$ consistently reduced the synaptic content of 2A-NMDARs (Fig. S3 *D* and *E*).

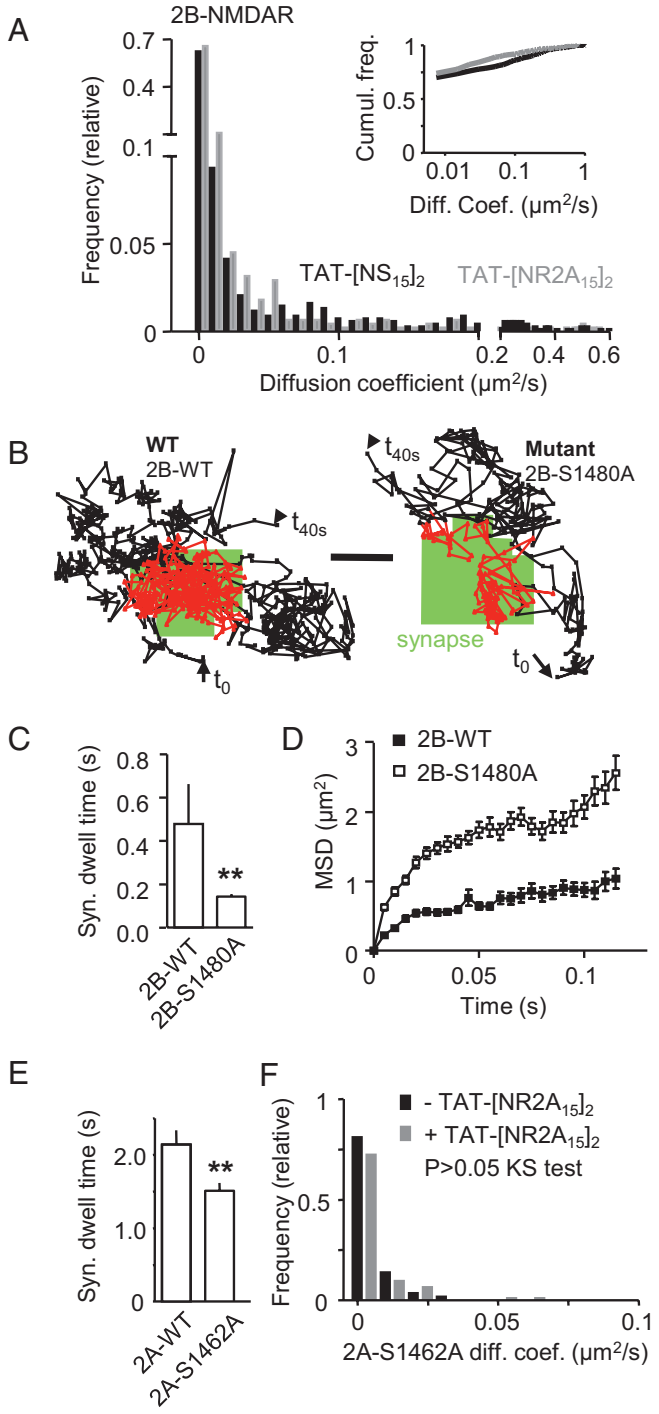

Fig. 2. TAT-$[NR2A_{15}]_2$ incubation does not affect native 2B-NMDARs or NR2A subunit mutant that does not bind to PDZ proteins. (*A*) Native 2B-NMDARs were tracked using QDs coupled to antibodies directed against an extracellular epitope of endogenous NR2B subunit in presence of TAT-$[NS_{15}]_2$ (n = 675 trajectories) or TAT-$[NR2A_{15}]_2$ (n = 442 trajectories). The frequency distribution (cumulative; *Upper Right*) of diffusion coefficients revealed that TAT-$[NR2A_{15}]_2$ did not significantly affect the diffusion of native 2B-NMDARs ($P > 0.05$, Mann–Whitney test). (*B*) The surface diffusion of recombinant 2B-NMDARs was assessed using recombinant flag-tagged NR2B subunits: WT (2B-WT) or mutant form (2B-S1480A) that does not bind PDZ proteins. These subunits were tracked using anti-Flag coupled QDs. Representative 40-s trajectories of anti-Flag QDs tracking 2B-WT (*Left*) or 2B-S1480A (*Right*). (Scale bar: 500 nm.) The starting and ending point are referred as t_0 and t_{40s}, respectively. The green areas correspond to synapses. (*C*) Synaptic dwell time was measured for 2B-NMDARs containing 2B-WT (n = 235 trajectories) or 2B-S1480A (n = 532 trajectories). Note the reduction in the time spent by 2B-S1480A within the synapse (**$P < 0.01$, t test). (*D*) Plot of the mean square displacement (MSD) versus time for synaptic receptors containing the subunit 2B-WT or 2B-S1480A. The curves exhibit a negative curvature characteristic of a confined behavior. Note the higher degree of confinement for 2B-WT subunits. (*E*) Synaptic dwell time was measured for 2A-NMDARs containing either 2A-WT (n = 487 trajectories) or mutant 2A-S1462A (n = 474 trajectories). Note the reduction in the time spent by the mutant within the synapse (**$P < 0.01$, t test). (*F*) The frequency distribution of diffusion coefficients of mutant 2A-S1462A in absence (n = 58 trajectories; black squares) or presence of TAT-$[NR2A_{15}]_2$ (n = 94 trajectories; gray squares). No significant difference was observed ($P > 0.05$, Mann–Whitney test).

NR2A-Derived Ligand Does Not Interfere with 2B-NMDAR, Kv Potassium Channel, or $GABA_A$ Receptor Surface Trafficking. The NR2 subunits are thought to associate with PSD-95 via a C-terminal 4-aa sequence, which is identical in NR2A and NR2B subunits. Other upstream amino acid sequences that differ between NR2A and NR2B subunits have also been implicated in PSD-95 binding (29), and there is some evidence that, at least for potassium channels, binding to PSD-95 tandem PDZ domains involves up to 12 C-terminal residues (30). Interestingly, the amino acid sequence homology decreases to only 60% after alignment of NR2A and NR2B subunit 15 C-terminal residues (Fig. S1). Although most studies on isolated PDZ domains and minimal peptides derived from the C-termini of binding partners tend to limit the ligand interacting residues to the C-terminal 4 aa, we anticipated that the native interactions might achieve higher specificity by engaging additional residues, constituting the rationale for using the last 15 aa of the NR2A subunit. We first analyzed the effect of TAT-$[NR2A_{15}]_2$ on native 2B-NMDAR surface diffusion [measured in young hippocampal cultured neurons that do not express 2A-NMDAR (25)]. Strikingly, TAT-$[NR2A_{15}]_2$ had no effect on the surface diffusion of native 2B-NMDARs (Fig. 2*A*). The diffusion coefficient distributions were superimposed, indicating that TAT-$[NR2A_{15}]_2$ did not affect the anchoring of 2B-NMDARs. Because the synaptic anchoring of 2B-NMDARs may not depend on the interaction with PDZ proteins, we compared the surface trafficking of NR2B WT (2B-WT) and a NR2B mutant (i.e., 2B-S1480A), which does not coimmunoprecipitate with PSD-95 (9). The diffusion coefficient was significantly higher for 2B-S1480A (median of 0.57 $\mu m^2/s$, IQR of 0.24–1.08 $\mu m^2/s$, n = 694 trajectories) than for 2B-WT (median of 0.32 $\mu m^2/s$, IQR of 0.13–0.69 $\mu m^2/s$, n = 344 trajectories) and the synaptic dwell time, defined as the mean time spent by a mobile receptor in the synaptic area, was significantly higher for 2B-WT compared with 2B-S1480A (Fig. 2*C*). Both 2B-WT and 2B-S1480A were confined within the synapse but to a significantly lower degree for 2B-S1480A (Fig. 2*D*). These results demonstrate that the synaptic retention of surface 2B-NMDARs is dynamically regulated by the interaction with PDZ proteins (9) and insensitive to TAT-$[NR2A_{15}]_2$ ligand. In addition, incubating the neurons with TAT-$NR2B_{15}$ (5 μM, 10 min) that mimics the last 15 aa of the NR2B subunit C terminus increased the surface diffusion of synaptic 2B-NMDARs without affecting the one of 2A-NMDARs (Fig. S4), consistent with previous biochemical reports using similar ligands (23, 24). Finally, a monovalent ligand containing only the last 6 aa of the NR2 C-terminus sequence (TAT-$NR2X_{15}$), which is identical for NR2A and NR2B subunits, increased the surface diffusion of both 2A- and 2B-NMDARs (Fig. S5), indicating that the PDZ binding sequence (last few amino acids of the C terminus) is indeed necessary to anchor the receptor in the synapse, and upstream amino acid sequence(s) provide a specificity motif for NR2 subunit.

To further test the specificity of the ligand, we then reasoned that if TAT-$[NR2A_{15}]_2$ competes specifically against the NR2A

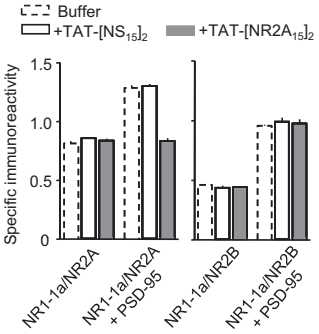

Fig. 3. TAT-$[NR2A_{15}]_2$ specifically blocks the interaction between PSD-95 and NR2A subunit. HEK 293 cells were cotransfected in triplicate with NR1-1a/NR2A or NR1-1a/NR2B with or without PSD-95 and cell surface expressed NMDARs measured by ELISA using either anti-NR2A 44–58 Cys or anti-NR2B 46–60 Cys affinity-purified antibodies. The results are expressed as the ratio of absorbance and expressed as the means ± SEM (n = 2 independent transfections for each combination). As previously shown, PSD-95 enhanced cell surface delivery of 2A- and 2B-NMDARs. These effects were then examined after incubation with TAT-$[NS_{15}]_2$ (10 μM; open bar) or TAT-$[NR2A_{15}]_2$ (10 μM; gray bar). Note that PSD-95 failed to increase surface 2A-NMDAR expression in the presence of TAT-$[NR2A_{15}]_2$.

C-terminal domain for the binding to its PDZ proteins, it would have no additional effect on the diffusion of 2A-NMDARs containing a 2A-S1462A mutation in the C terminus that prevents NR2A/PSD-95 coimmunoprecipitation (co-IP) (9). The 2A-S1462A displayed a threefold higher surface diffusion ($P <$ 0.001) and 1.4-fold shorter dwell time (Fig. 2*E*) than WT 2A-NMDARs. TAT-$[NR2A_{15}]_2$ did not increase the surface diffusion of 2A-S1462A (Fig. 2*F*), indicating that the TAT-$[NR2A_{15}]_2$-induced increase in 2A-NMDAR surface diffusion was occluded by the 2A-S1462A-induced increase in 2A-NMDAR surface diffusion. We then tested the specificity of TAT-$[NR2A_{15}]_2$ on other membrane proteins by imaging the surface trafficking of the native potassium channel Kv1.3, endogenously expressed in hippocampal neurons (31), because its C terminus contains a PDZ binding site similar to those of NR2A and NR2B subunits (Fig. S6*A*) (32). Remarkably, TAT-$[NR2A_{15}]_2$ produced no change in the diffusion pattern, the mobile fraction, the global diffusion coefficient, or the surface distribution of Kv1.3 channels (Fig. S6 *B–E*). Thus, although NR2A and Kv1.3 channel bind PDZ site with similar affinities (32) and exhibit a high similarity in their C-terminus amino acid sequence, TAT-$[NR2A_{15}]_2$ specifically acts on surface 2A-NMDARs and not on surface Kv1.3 channel. In addition, we report that TAT-$[NR2A_{15}]_2$ does not impact on the surface $GABA_A$ receptor (Fig. S6*F*), which is not anchored in synapse by a PDZ domain-binding motif (33).

Interaction Between NR2A Subunits and PSD-95 Is Specifically Disrupted by the NR2A Ligand. Because the PDZ-containing scaffolding proteins change during development, i.e., PSD-95 is the dominant scaffolding protein in mature neurons and SAP102 is the dominant scaffolding protein in immature neurons, the possibility that the TAT-$[NR2A_{15}]_2$ ligand better interacts with certain PDZ proteins remains to be tested. For this, we first measured, from forebrain homogenates, the impact of the NR2A ligand on the interaction between PSD-95 and NR2A or NR2B subunits using co-IP. The PSD-95/2A subunit interaction was specifically affected by the ligand whereas the PSD-95/2B subunit interaction remains unaffected (Fig. S7). Furthermore, we used a heterologous cell system to further determine the impact of the ligand on the interaction between NR2 subunit and the most abundant PDZ proteins, PSD-95. In heterologous cells, 2A- and 2B-NMDARs coimmunoprecipitate with the four PSD-95 MAGUK family of scaffolding proteins (34). In addition, PSD-95 enhances 2A- and 2B-NMDAR cell surface expression through a process that requires the NR2 C terminus sequence -ESDV (34). To test the specificity of TAT-$[NR2A_{15}]_2$ on 2A- and 2B-NMDAR trafficking, we then measured the effect of PSD-95 on cell surface 2A- or 2B-NMDAR expression, as previously described (34). We first observed that either TAT-$[NS_{15}]_2$ or TAT-$[NR2A_{15}]_2$ had no effect per se on the basal expression of the subunit (Fig. 3). PSD-95 enhanced the cell surface expression of both 2A- and 2B-NMDARs (Fig. 3). The incubation with TAT-$[NR2A_{15}]_2$ completely blocked the PSD-95-induced 2A-NMDAR surface expression, whereas TAT-$[NR2A_{15}]_2$ had no effect on PSD-95-induced 2B-NMDAR surface expression (Fig. 3). In all conditions, TAT-$[NS_{15}]_2$ incubation had no significant effect on the PSD-95-induced NR2-NMDAR surface expression. All together, these data demonstrate, in neuronal and heterologous systems, that the TAT-$[NR2A_{15}]_2$ divalent ligand specifically blocks the interaction between 2A-NMDARs (no effect on 2B-NMDARs) and the most abundant protein of the postsynaptic density, PSD-95.

Rapid Redistribution of 2A- and 2B-NMDARs in Excitatory Synapses. As TAT-$[NR2A_{15}]_2$ specifically destabilizes synaptic 2A-NMDARs, we investigated the functional consequences of such an effect by first measuring NMDAR-mediated synaptic currents. We report that, in the presence of $[NR2A_{15}]_2$ (within recording pipette), the kinetics of NMDAR miniature excitatory postsynaptic currents (mEPSCs) were significantly increased whereas AMPAR mEPSC remained unchanged (Fig. S8). We then recorded evoked NMDA excitatory postsynaptic currents (eEPSC) from CA1 pyramidal neurons (P16–20; Fig. 4*A*) and found that a 15- to 20-min dialysis of $[NR2A_{15}]_2$ significantly increased the Ro 25-6981 (NR2B subunit antagonist, 1 μM)-induced inhibition of NMDAR current (Fig. 4*A*), consistent with an increased contribution of 2B-NMDARs to synaptic currents. Interestingly, the amplitude of both mEPSCs and eEPSCs remained unchanged in the presence of $[NR2A_{15}]_2$, indicating that the $[NR2A_{15}]_2$-induced removal of 2A-NMDARs from synapse was compensated by the insertion of other NMDARs with slower kinetics (Fig. 4*B*). To gain insight in the NR2-NMDAR trafficking at identified synapses, the fluorescence intensity of surface NR2A (SEP-NR2A) and NR2B (SEP-NR2B) subunits was measured over time before and after incubation with TAT-$[NS_{15}]_2$ or TAT-$[NR2A_{15}]_2$ (Fig. 4*C*). Synaptic and extrasynaptic NMDARs were distinguished by coexpressing the synaptic marker Homer 1C-DsRed. First, the intensity of extrasynaptic surface NMDARs (SEP-NR1, SEP-NR2A, SEP-NR2B) was not significantly altered by the presence of TAT-$[NS_{15}]_2$ or TAT-$[NR2A_{15}]_2$. Within synapses, the intensity of 2A-NMDAR clusters was decreased as demonstrated by the significant left shift of the cluster distributions ($P <$ 0.001; Fig. 4*D*) or by the significant decrease of average values (Fig. 4*E*). Surprisingly, under the same conditions the intensity of 2B-NMDAR synaptic clusters was increased significantly (e.g., right shift of the distribution; $P <$ 0.001; Fig. 4 *D* and *E*). The effect was observed 15 to 20 min after the ligand incubation and was stable over time. In such mature synapses, TAT-$[NR2A_{15}]_2$ reduced the surface diffusion of synaptic 2B-NMDARs and increased their synaptic dwell time, consistent with a higher retention of these receptors. These data demonstrate thus that 2A- and 2B-NMDARs rapidly redistribute within synaptic areas. In addition, displacing 2A-NMDARs out of synapses by preventing the interaction of 2A-NMDARs and PDZ proteins is compensated by the increase contribution of other NMDAR subtypes, indicating that an unexpected level of specificity between NR2 subunits and PDZ proteins is present in postsynaptic densities.

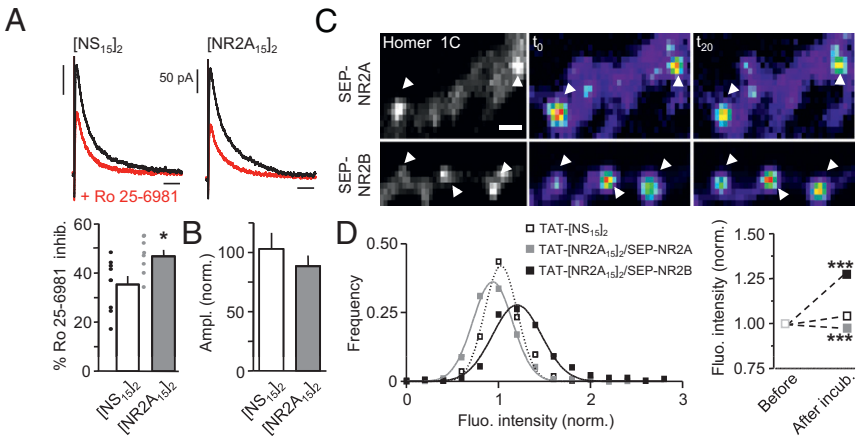

Fig. 4. Dynamic regulation of surface 2A- and 2B-NMDAR content in postsynaptic areas. (*A*) Evoked NMDAR EPSCs (recorded at +30 mV) averaged at 0 to 2 min (black trace) or 18 to 20 min (red trace) after dialysis with Ro 25-6981 (1 μM, 2B-NMDAR antagonist; *Left*). (Horizontal scale bar: 100 ms.) The Ro 25-6981 incubation significantly reduced the NMDAR eEPSC amplitude (*Right*). In te presence of $[NS_{15}]_2$ (n = 9 neurons) or $[NR2A_{15}]_2$ (n = 8 neurons), Ro 25-6981 reduced the NMDAR eEPSC amplitude by 35% and 47%, respectively. (*B*) The amplitude (normalized) of NMDAR eEPSCs remained stable in presence of $[NR2A_{15}]_2$ ligand ($[NS_{15}]_2$, n = 6 neurons; $[NR2A_{15}]_2$, n = 7 neurons). (*C*) The fluorescence intensity of synaptic SEP-NR2A (*Upper*) and SEP-NR2B (*Lower*) clusters colocalized with Homer 1C was followed over a period of 20 min after acute addition of 5 μM of TAT-$[NR2A_{15}]_2$ (Scale bar: 1 μm.) (*D*) *Left*: Frequency distribution of the fluorescence intensity of SEP-NR2A and SEP-NR2B clusters after 20 min in the presence of TAT-$[NS_{15}]_2$ or TAT-$[NR2A_{15}]_2$. The Gaussian fit is centered on 1 after incubation with TAT-$[NS_{15}]_2$ (n = 563 clusters; dashed black line) indicating that the receptor content within the cluster did not change over time. Note the shift of the curve toward the left for SEP-NR2A (n = 451 clusters; solid gray line) and toward the right for SEP-NR2B (n = 309 clusters; full black line) after the 20 min incubation with TAT-$[NR2A_{15}]_2$ showing, respectively, a decrease and an increase in the receptor content. *Right*: Normalized mean fluorescence intensity of the clusters before and after a 20-min incubation with TAT-$[NS_{15}]_2$ or TAT-$[NR2A_{15}]_2$ ($P < 0.001$, paired t test).

Discussion

Although synaptic NR2-NMDARs play a key role in synaptic refinement (2), the molecular mechanisms as well as the dynamics that govern their surface distribution and rapid trafficking are largely unknown. To shed new light on this issue, we developed a biomimetic divalent ligand that acutely and efficiently blocks the interaction between PDZ proteins and native 2A-NMDARs (enriched at synapses). We unravel an unexpected role of the divalent arrangement of the NR2 subunits in providing efficient anchoring within synapses and strengthen the need to dynamically study such interactions in native conditions. Indeed, by using mono- or divalent ligands, we now identified that the binding efficacy is highly dependent on the divalent structure of the 2A-NMDAR complex, and the specific binding of 2A-NMDAR (versus 2B-NMDAR for instance) relies on amino acid sequence(s) upstream to the C terminus, whereas the last C terminus amino acids are implicated in the direct binding to PDZ scaffold proteins (Fig. S9). Thus, NR2 subunits associate with PDZ proteins via a C-terminal 4-aa sequence (7–10), which is identical in NR2A and NR2B subunits, and other upstream amino acids that are within 15 aa of the C terminus, and as previously proposed, in more upstream sequences (29). Although the binding mechanism of these domains remains poorly understood (35), it suggests that 2A- or 2B-NMDARs are engaged in different sets of interactions within the scaffold environment. Consistently, the NR2A-ligand-induced rapid exit of 2A-NMDARs from postsynaptic densities was paralleled by a compensatory increase in 2B-NMDAR content, indicating that the 2A/2B-NMDAR synaptic ratio is dynamically regulated. Functionally, long-term potentiation of hippocampal synapses has been associated with a rapid change in the synaptic content in 2A and 2B-NMDARs (36), consistent with a dynamic redistribution of surface 2A- and 2B-NMDARs around the synaptic area. Thus, understanding the rules that govern NR2-NMDAR surface distribution and, most importantly, their dynamic retention in the postsynaptic density will surely shed new lights on the nanodomain organization of NMDARs and the fine tuning of NMDAR-dependent forms of synaptic adaptations in physiological and pathological paradigms.

Materials and Methods

Complete discussions of ligand synthesis, cell culture, immunocytochemistry, synaptic live cell staining, protein expression, single particle (QD) tracking, fluorescence recovery after photobleaching (FRAP), electrophysiology, immunoprecipitation, and in vitro cell surface assays are in *SI Materials and Methods*. The transduction and cell distribution of the ligand are detailed in Fig. S10. The impact of the ligand and its vehicle on receptor trafficking is detailed in Fig. S11.

ACKNOWLEDGMENTS. We thank Laurent Ladépêche, Beatrice Tessier, Arnaud Frouin, and Christophe Blanchet for technical assistance; Robert Wenthold (National Institutes of Health, Bethesda, MD) for providing NR2 cDNA plasmids and constructive discussions; and Antoine Triller [Ecole Normale Superieure (ENS), Paris] for providing antibody. This work was supported by Centre National de la Recherche Scientifique/Agence Nationale de la Recherche Grant JC08_329238 (to L.G.), Chem-Traffic (M.S. and D.C.), Human Frontier Science Program Grant MRGP0007/2006-C (to B.I., M.S., and D.C.), Fondation pour la Recherche Médicale (L.B., D.C.,and L.G.), Conseil Régional d'Aquitaine, Marie Curie postdoctoral fellowship (PICK-CPP to M.S.), Ministère de l'Enseignement Supérieur et de la Recherche, European Research Council Advanced Research Grant Nano-Dyn-Syn (to D.C.), and the UK Biotechnology and Biological Sciences Research Council (F.A.S.).

1. Cull-Candy SG, Leszkiewicz DN (2004) Role of distinct NMDA receptor subtypes at central synapses. *Sci STKE* 2004:re16.
2. Yashiro K, Philpot BD (2008) Regulation of NMDA receptor subunit expression and its implications for LTD, LTP, and metaplasticity. *Neuropharmacology* 55:1081–1094.
3. Chen BS, Roche KW (2007) Regulation of NMDA receptors by phosphorylation. *Neuropharmacology* 53:362–368.
4. Lau CG, Zukin RS (2007) NMDA receptor trafficking in synaptic plasticity and neuropsychiatric disorders. *Nat Rev Neurosci* 8:413–426.
5. Pérez-Otaño I, Ehlers MD (2005) Homeostatic plasticity and NMDA receptor trafficking. *Trends Neurosci* 28:229–238.
6. Wenthold RJ, Prybylowski K, Standley S, Sans N, Petralia RS (2003) Trafficking of NMDA receptors. *Annu Rev Pharmacol Toxicol* 43:335–358.
7. Kornau HC, Schenker LT, Kennedy MB, Seeburg PH (1995) Domain interaction between NMDA receptor subunits and the postsynaptic density protein PSD-95. *Science* 269:1737–1740.
8. Mohrmann R, Köhr G, Hatt H, Sprengel R, Gottmann K (2002) Deletion of the C-terminal domain of the NR2B subunit alters channel properties and synaptic targeting

of N-methyl-D-aspartate receptors in nascent neocortical synapses. *J Neurosci Res* 68: 265–275.
9. Prybylowski K, et al. (2005) The synaptic localization of NR2B-containing NMDA receptors is controlled by interactions with PDZ proteins and AP-2. *Neuron* 47: 845–857.
10. Cui H, et al. (2007) PDZ protein interactions underlying NMDA receptor-mediated excitotoxicity and neuroprotection by PSD-95 inhibitors. *J Neurosci* 27:9901–9915.
11. Barria A, Malinow R (2002) Subunit-specific NMDA receptor trafficking to synapses. *Neuron* 35:345–353.
12. Chung HJ, Huang YH, Lau LF, Huganir RL (2004) Regulation of the NMDA receptor complex and trafficking by activity-dependent phosphorylation of the NR2B subunit PDZ ligand. *J Neurosci* 24:10248–10259.
13. Mori H, et al. (1998) Role of the carboxy-terminal region of the GluR epsilon2 subunit in synaptic localization of the NMDA receptor channel. *Neuron* 21:571–580.
14. Sprengel R, et al. (1998) Importance of the intracellular domain of NR2 subunits for NMDA receptor function in vivo. *Cell* 92:279–289.
15. Thomas CG, Miller AJ, Westbrook GL (2006) Synaptic and extrasynaptic NMDA receptor NR2 subunits in cultured hippocampal neurons. *J Neurophysiol* 95: 1727–1734.
16. Steigerwald F, et al. (2000) C-Terminal truncation of NR2A subunits impairs synaptic but not extrasynaptic localization of NMDA receptors. *J Neurosci* 20:4573–4581.
17. Köhr G, et al. (2003) Intracellular domains of NMDA receptor subtypes are determinants for long-term potentiation induction. *J Neurosci* 23:10791–10799.
18. Neyton J, Paoletti P (2006) Relating NMDA receptor function to receptor subunit composition: Limitations of the pharmacological approach. *J Neurosci* 26:1331–1333.
19. Aarts M, et al. (2002) Treatment of ischemic brain damage by perturbing NMDA receptor- PSD-95 protein interactions. *Science* 298:846–850.
20. Gardoni F, et al. (2006) A critical interaction between NR2B and MAGUK in L-DOPA induced dyskinesia. *J Neurosci* 26:2914–2922.
21. Lim IA, Merrill MA, Chen Y, Hell JW (2003) Disruption of the NMDA receptor-PSD-95 interaction in hippocampal neurons with no obvious physiological short-term effect. *Neuropharmacology* 45:738–754.
22. Stephenson FA, Cousins SL, Kenny AV (2008) Assembly and forward trafficking of NMDA receptors (review). *Mol Membr Biol* 25:311–320.
23. Sainlos M, Iskenderian WS, Imperiali B (2009) A general screening strategy for peptide-based fluorogenic ligands: Probes for dynamic studies of PDZ domain-mediated interactions. *J Am Chem Soc* 131:6680–6682.
24. Groc L, et al. (2007) Surface trafficking of neurotransmitter receptor: comparison between single-molecule/quantum dot strategies. *J Neurosci* 27:12433–12437.
25. Groc L, et al. (2006) NMDA receptor surface mobility depends on NR2A-2B subunits. *Proc Natl Acad Sci USA* 103:18769–18774.
26. Tovar KR, Westbrook GL (2002) Mobile NMDA receptors at hippocampal synapses. *Neuron* 34:255–264.
27. Zhao J, et al. (2008) Synaptic metaplasticity through NMDA receptor lateral diffusion. *J Neurosci* 28:3060–3070.
28. Tovar KR, Westbrook GL (1999) The incorporation of NMDA receptors with a distinct subunit composition at nascent hippocampal synapses in vitro. *J Neurosci* 19: 4180–4188.
29. Cousins SL, Kenny AV, Stephenson FA (2009) Delineation of additional PSD-95 binding domains within NMDA receptor NR2 subunits reveals differences between NR2A/PSD-95 and NR2B/PSD-95 association. *Neuroscience* 158:89–95.
30. Pegan S, et al. (2007) NMR studies of interactions between C-terminal tail of Kir2.1 channel and PDZ1,2 domains of PSD95. *Biochemistry* 46:5315–5322.
31. Grosse G, et al. (2000) Expression of Kv1 potassium channels in mouse hippocampal primary cultures: Development and activity-dependent regulation. *J Neurosci* 20: 1869–1882.
32. Lim IA, Hall DD, Hell JW (2002) Selectivity and promiscuity of the first and second PDZ domains of PSD-95 and synapse-associated protein 102. *J Biol Chem* 277:21697–21711.
33. Fritschy JM, Harvey RJ, Schwarz G (2008) Gephyrin: Where do we stand, where do we go? *Trends Neurosci* 31:257–264.
34. Cousins SL, Papadakis M, Rutter AR, Stephenson FA (2008) Differential interaction of NMDA receptor subtypes with the post-synaptic density-95 family of membrane associated guanylate kinase proteins. *J Neurochem* 104:903–913.
35. Ryan TJ, Emes RD, Grant SG, Komiyama NH (2008) Evolution of NMDA receptor cytoplasmic interaction domains: implications for organisation of synaptic signalling complexes. *BMC Neurosci* 9:6.
36. Bellone C, Nicoll RA (2007) Rapid bidirectional switching of synaptic NMDA receptors. *Neuron* 55:779–785.